LANGMUIR Article
Cite This: Langmuir 2019, 35, 16466−16475
pubs.acs.org/Langmuir

Site-Specific and Covalent Immobilization of His-Tagged Proteins via Surface Vinyl Sulfone−Imidazole Coupling

Mingyang Li,[†,‡] Fang Cheng,*[,†,‡] Haoqiang Li,[∥] Weiwei Jin,[∥] Chen Chen,[§] Wei He,[†,‡] Gang Cheng,[⊥] and Qing Wang[†,‡]

[†]State Key Laboratory of Fine Chemicals, [‡]School of Chemical Engineering, and [§]School of Bioengineering, Dalian University of Technology, Dalian, Liaoning 116023, China

[∥]Hangzhou HealSun Biopharm Co., Ltd., Hangzhou, Zhejiang 735400, China

[⊥]Department of Chemical Engineering, University of Illinois at Chicago, Chicago, Illinois 60607, United States

Supporting Information

ABSTRACT: Site-specific immobilization of proteins on a surface has been a long-lasting challenge in the fields of biosensing and biotechnology because of the need for improving the biological activity of immobilized protein via the maximal exposure of its bioactive domain. Herein, we reported a new site-specific immobilization method for His-tagged proteins onto a vinyl sulfone (VS)-bearing surface in a covalent manner. X-ray photoelectron spectroscopy characterization indicated the specificity of the addition reaction of the imidazole group in histidine on the VS-bearing surface at pH 7.0. Solution-based experiments were carried out to verify the reaction priority of the imidazole residue of histidine with the VS group at neutral conditions. The real-time immobilization process of two His-tagged proteins (HaloTag-6His and anti-HER2 Fab-6His) on surfaces presenting VS, preactivated carboxyl, and NTA groups were studied by quartz crystal microbalance. Compared to the existing methods utilizing covalent (NHS/EDC activated carboxyl) and coordinate (Ni^{2+}-NTA) linking, our method offers two significant advantages for protein immobilization: high density and high specificity. The orientation of the two His-tagged proteins on the VS-bearing surface was confirmed by an enzyme-linked assay and an $HER2^{+}$ liposome binding experiment. Our method of site-specific immobilization of His-tagged proteins is efficient and straightforward, which would be helpful to expand the applications of recombinant proteins in enzyme immobilization, biosensor and array fabrication, and drug delivery system.

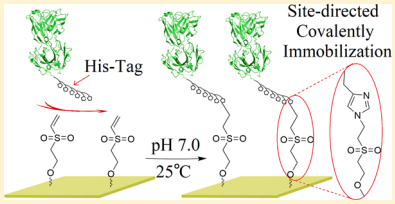

INTRODUCTION

Well-controlled protein orientation has been proven to improve both biosensing sensitivity and enzymatic reactivity effectively.[1−3] It is due to the maximal exposure of the binding domain or bioactive site to target molecules in solution. To realize a specific orientation, the proteins of interest are designed to be anchored on a substrate surface in a site-specific manner.[4−6] Through either physical or chemical binding of proteins onto the surface, a variety of methods have been developed, and the resulting enhancements in the activities of the immobilized proteins were observed. For example, it was reported that the orientation of IgG on the surfaces of surface plasmon resonance (SPR) chips[7] and nanoparticles[8,9] could be controlled through electrostatic interactions, thus improving the sensitivity of SPR and delivery of nanoparticles. The unique interaction between the adjacent diols in carbohydrate moieties and boronic acids has been used for the site-specific immobilization of glycoproteins.[10,11] Although the specific binding and the simple steps have been reported, these methods are limited to a few of natural proteins.

For the site-specific immobilization, the recombinant protein engineering approach is a powerful tool to introduce an affinity tag at the N- or C-terminus of a protein.[12−14] Among a variety of affinity tags, the hexahistidine tag (His-Tag) has been widely used because of its short motif and minimal interference of protein expression and folding[15−17] (Scheme 1a). However, the intrinsic reversibility of coordination binding that is mediated by a coordinate bond would cause a slow and continuous dissociation of the immobilized His-tagged proteins into solution.[18] Therefore, a more stable immobilization method of His-tagged protein is highly desirable.

Compared to other active amino acid residues in a protein for immobilization, for example, lysine and arginine, the imidazole side chain in histidine has a lower pK_a (6.04),[19] which is deprotonated even at a neutral or slightly acidic condition.[20] Thus, the imidazole group can function as a nucleophilic agent in a Michael-type reaction,[21,22] which has been widely used for bioconjugation and polymer synthesis due to its high efficiency and mild reaction conditions. In addition, rather than a single histidine, His-Tag would have the significantly enhanced reactivity. Recently, two electrophilic reagents, that is, PEG-*mono*-sulfone reagent[20,23] (Scheme 1b) and thiophosphorodichloridate[24] (Scheme 1c), are employed to demonstrate the site-specific conjugation of His-tagged

Received: September 18, 2019
Revised: November 15, 2019
Published: November 22, 2019

DOI: 10.1021/acs.langmuir.9b02933
Langmuir 2019, 35, 16466−16475

Scheme 1. Site-Specific Immobilization and Conjugation of His-Tagged Proteins[a]

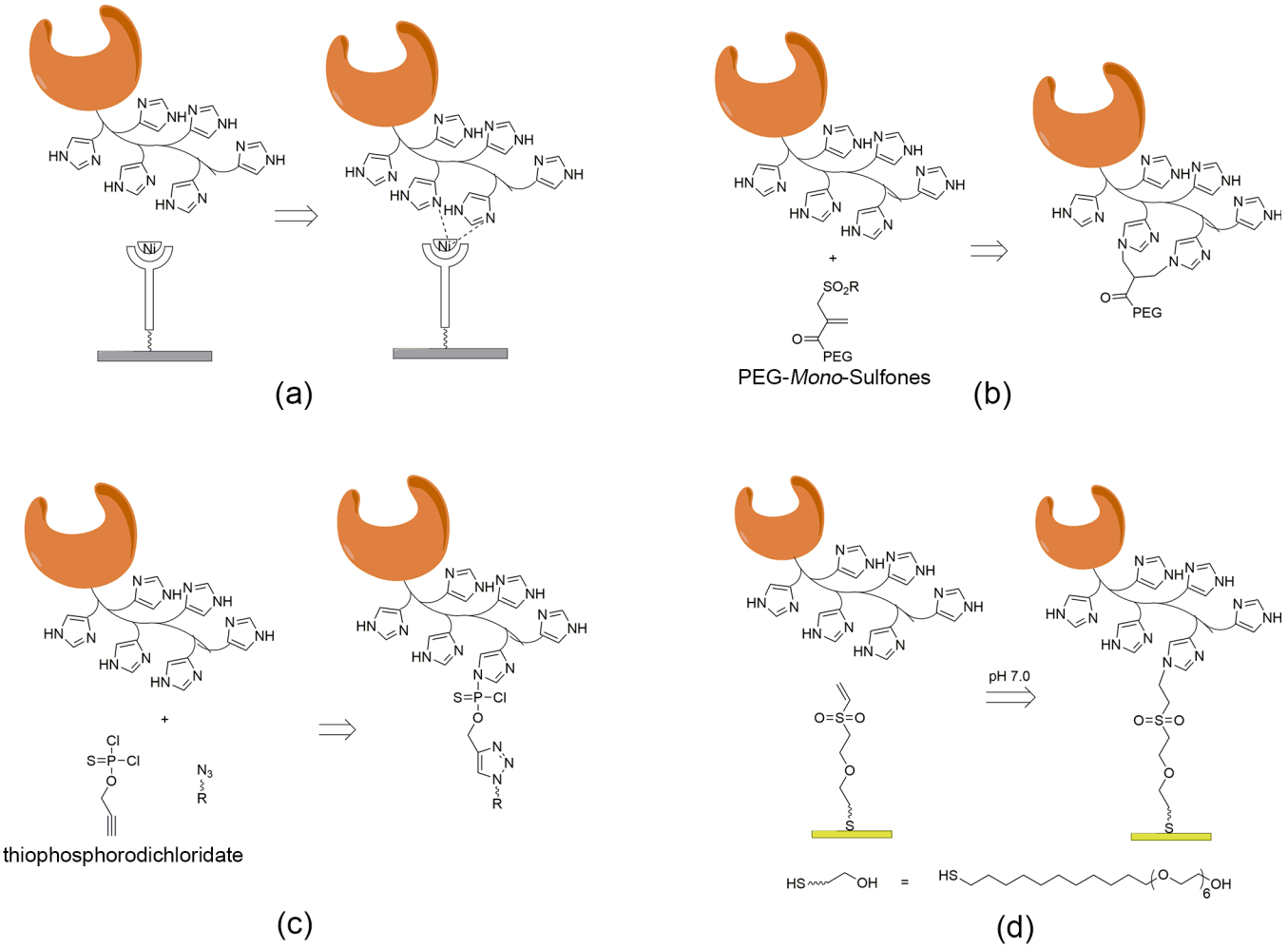

[a]Site-specific immobilization of His-tagged proteins using a coordinate linking method on the Ni^{2+}-NTA surface (a) and site-specific conjugation of His-tagged proteins using PEG-*mono*-sulfones (b) and thiophosphorodichloridate (c) in solution, and site-specific immobilization of His-tagged proteins onto VS-bearing surface (d).

proteins in solution. According to the reaction specificity and efficiency, the conjugation methods are applausive. Unfortunately, the site-specific immobilization of His-tagged proteins onto surfaces using such electrophilic reactions has not been unexploited.

Herein, we aim to develop a covalent site-specific immobilization method of the His-tagged protein onto a vinyl sulfone (VS)-bearing surface (Scheme 1d). VS-bearing surface was prepared by introducing VS groups onto hydroxyl-terminated self-assembled monolayers (SAMs) through organocatalysis.[25] On the as-prepared VS-bearing SAM surface, XPS was used to examine the surface reaction with the histidine and lysine in which both α-amine groups are protected. To compare the reactivity and specificity of the imidazole side chain in histidine and the ω-amine in lysine, ^{13}C NMR was used to analyze the solution-based reaction of a VS-bearing compound with histidine and lysine containing the protected α-amine group. Subsequently, the amount and specificity of two His-tagged proteins, that is, HaloTag-6His and anti-HER2 Fab-6His, onto the VS-bearing surface was systematically studied by using quartz crystal microbalance (QCM). For the quantitative comparison, the kinetics of protein adsorption/desorption onto preactivated carboxyl-terminated and NTA surfaces are analyzed. Finally, the orientation of the two His-tagged proteins was assessed by an enzyme-linked immunosorbent assay and $HER2^+$ liposome binding experiments.

EXPERIMENTAL SECTION

Reagents and Materials. *N*-Alpha-(*tert*-butoxycarbonyl)-L-histidine (Boc-His), *N*-alpha-(*tert*-butoxycarbonyl)-L-lysine (Boc-Lys), D_2O, bovine serum albumin (BSA), divinyl sulfone (DVS), *N*-hydroxysuccinimide (NHS), and 1-(3-dimethylaminopropyl)-3-ethyl-carbodiimide hydrochloride (EDC) were purchased from Sigma (Milwaukee, USA). The oligopeptides of Boc-HHHHHH, RGD, and GGGRGDS were synthesized by GL Biochem Ltd. (Shanghai, China). Horseradish peroxidase (HRP) and TMB (3,3′,5,5′-tetramethylbenzidine) two-component substrate solution and streptavidin-6His were obtained from Solarbio Science & Technology Co., Ltd. (Beijing, China). Streptavidin was purchased from Thermo Fisher Scientific Inc. (USA). Anti-HER2 antibody was provided from Hangzhou HealSun Biopharm Co., Ltd. (Hangzhou, China). HaloTag coumarin ligand was purchased from Promega Biotech Co., Ltd. (USA). Hydroxy-EG_6-undecanethiol and carboxy-EG_6-undecanethiol were obtained from Dojindo Molecular Technologies (Tokyo, Japan). Triphenylphosphine (PPh_3) was purchased from Guangfu Fine Chemical Research Institute (Tianjin, China). Ethanol (HPLC grade) was purchased from Tedia (Fairfiele, USA). Other chemicals

DOI: 10.1021/acs.langmuir.9b02933
Langmuir 2019, 35, 16466−16475

were of analytical grade from local sources. All chemicals were used as received without further purification. Ultrapure water with an 18.2 MΩ·cm resistivity was used in all experiments.

Preparation of Au Substrates. The preparation of Au substrates was reported in our previous work.[25] Specifically, silicon wafers were immersed in piranha solution (a 3:1 mixture of 97% sulfuric acid and 30% hydrogen peroxide) for 30 min (caution: piranha solution reacts violently with most organic materials and must be handled with extreme care). Once the wafers were removed from piranha solution, they were rinsed with a copious amount of water and ethanol and then dried under a stream of nitrogen. Titanium (5 nm) and gold (45 nm) were sequentially deposited onto the cleaned silicon wafers (10 × 10 mm) using a Turbo sputter coater K575XD (Kent, U.K.).

Preparation of EG_6-OH SAMs. The Au substrates were cleaned in an ultraviolet (UV)/ozone cleaner for 30 min and rinsed intensively with ethanol. The cleaned Au substrates were immersed in an ethanolic solution of hydroxy-EG_6-undecanethiol (0.2 mg/mL) for 24 h at 25 °C. The resulting EG_6-OH SAM samples were then washed with a copious amount of ethanol and dried under a stream of nitrogen.

Preparation of VS-Bearing Surfaces. The preparation method of the VS-bearing surface starting with the OH surface was reported previously.[25] Briefly, the as-prepared EG_6-OH SAM samples were immersed in DVS solution (1 M in acetonitrile containing 10 mM PPh_3 as a catalyst) and incubated at 25 °C for 6 h. The samples were then washed with copious amounts of acetonitrile and dried under a stream of nitrogen. The sample surfaces bearing VS groups were named as VS-EG_6 surface.

Preparation of Carboxy-EG_6 Surfaces. The cleaned Au substrates were immersed in an ethanolic solution of carboxy-EG_6-undecanethiol (0.2 mg/mL) at 25 °C for 24 h. The substrates were then activated in NHS/EDC solution (20 mM NHS, 40 mM EDC, 20 mM PB, pH 6.5) for 1 h in an ice bath. At last, the surfaces were washed with copious amounts of ultrapure water and dried under a stream of nitrogen. The sample surfaces bearing NHS activated carboxyl groups were named as Carboxy-EG_6 surface.

Preparation of NTA-EG_6 Surfaces. The NTA modification method of VS surface refers to our previous work.[26] After washing with acetonitrile and drying under a stream of nitrogen, the as-prepared VS-bearing surface was dipped into a HEPES buffer (pH 8.5) with 20 mM ab-NTA at 25 °C for 12 h. The substrates were then blocked with 50 mM ethanolamine (HEPES buffer, pH 8.5). Then, the substrates were dipped into $NiCl_2$ solution (0.1 M in water) for 30 min at 25 °C. At last, the surfaces were washed with copious amounts of ultrapure water and dried under a stream of nitrogen. The prepared substrates were named as NTA-EG_6 surface.

X-ray Photoelectron Spectroscopy (XPS) Characterization. XPS measurements were performed on a Thermo Scientific ESCALAB 250Xi X-ray photoelectron spectrometer (Waltham, MA) equipped with a monochromatic Al Kα radiation. The survey spectra and high-resolution spectra of C 1s, N 1s, O 1s, and S 2p were scanned at pass energies of 100.0 and 20.0 eV, respectively. All XPS data were carried out at a photoelectron takeoff angle of 90°. All binding energies were referenced to the C 1s peak calibrated at 285.0 eV. Each sample was tested with a spot size of 900 μm.

Solution-Based Reactions. VS-EG_3-OMe (10 mM), Boc-His (20 mM), and Boc-Lys (20 mM) were mixed in the pH 7.0 PB buffer at 25 °C for 48 h. The samples were prepared by drying in a lyophilizer and then dispersed in D_2O. ^{13}C NMR spectrum was collected by using an Avance II400 MHz spectrometer (Bruker, Switzerland).

Real-Time Measurement of Protein Immobilization Behaviors Using Quartz Crystal Microbalance (QCM). The real-time monitor of protein immobilization was conducted on a 5 MHz QCM (Q-sense E1, Biolin Scientific, Sweden). The flow rate was set at 50 μL/min, and the QCM frequency changes were monitored over time at 25 °C. Before the protein immobilization, carboxy-EG_6 chips are treated with NHS/EDC solution (20 mM NHS, 40 mM EDC) for 30 min, and NTA-EG_6 chips are treated with $NiCl_2$ solution (0.1 M in water) for 10 min. Both preactivated chips were thoroughly rinsed with ultrapure water before use.

For protein immobilization, the following protocol was used: an equilibrate step with PB buffer (20 mM, pH 7.0) for 10 min, followed by the protein immobilization step with 0.5 or 0.05 mg/mL protein solutions (HaloTag-6His or anti-HER2 Fab-6His, 20 mM PB buffer, pH 7.0) and a washing step with PB buffer (20 mM, pH 7.0). BSA solution (0.5 mg/mL, 20 mM PB buffer, pH 7.0) was selected as a control. The prepared anti-HER2 Fab-6His surfaces based on VS-bearing, Carboxyl-EG_6, and NTA-EG_6 chips will be used in adsorption equilibrium experiments. As the protein solution flowed over chip surfaces, the QCM frequency would decrease and the mass of adsorbed protein can be estimated according to Sauerbrey equation (eq 1)

$$\Delta m = -C\Delta f\Big|_n \tag{1}$$

$$D = \Delta m\Big|_M \tag{2}$$

where Δm denotes the binding mass of protein on the sensor chips, C = 17.7 ng Hz^{-1} cm^{-2} is a constant for the 5 MHz quartz crystal chips used in these experiments, Δf denotes the QCM frequency response, n denotes the overtone number, D denotes the molar density of immobilized proteins, and M denotes the molar mass of proteins (the molecular weights of HaloTag-6His and anti-HER2 Fab-6His are determined to be 34.4 and 48.1 kDa by MALDI-TOF-MS analysis, respectively).

Enzyme-Linked Assay. For HRP assay, the VS-bearing, Carboxyl-EG_6, and NTA-EG_6 surfaces were prepared on the Au substrates (10 × 10 mm) surface by using the above methods. Before the protein immobilization, Carboxy-EG_6 surfaces are treated with NHS/EDC solution (20 mM NHS, 40 mM EDC) for 30 min, and NTA-EG_6 surfaces are treated with $NiCl_2$ solution (0.1 M in water) for 10 min. Both preactivated surfaces were thoroughly rinsed with ultrapure water before use.

The three types of sample surfaces were transferred into 0.5 mg/mL HalTag-6His solution (20 mM PB buffer, pH 7.0) for 12 h at 25 °C. The unreacted VS groups were blocked with a freshly prepared solution of 20 mM 2-aminoethanol (10 mM HEPES, pH 8.0) for 6 h at 25 °C. Then, the three types of sample surfaces were blocked with 1% BSA solution (20 mM PBS, pH 7.4) at 4 °C for 12 h. Surfaces were then washed with PBS buffer (20 mM, pH 7.4) and incubated with Cl-linked HRP at 0.1 mg/mL at 25 °C for 1 h. After washing with PBS buffer (20 mM, pH 7.4), the sample surfaces were placed in a 24-well plate. Then, 500 μL/well of TMB two-component substrate solutions was added and incubated at 25 °C for 15 min. Enzymatic reactions were stopped by adding 500 μL of 1 M H_2SO_4, and the absorbance was measured at 450 nm using a microplate reader (BioTek, USA). The HaloTag-6His-conjugated VS-bearing surface incubated with unlabeled HRP was selected as a control. The Au substrate in the absence of surface modification was used as a blank control. All the measurements were repeated three times. The results were reported as a mean ± standard deviation.

Adsorption Equilibrium of Cell Membrane-Derived Liposome by QCM. Cell membrane-derived liposome binding experiments were conducted by QCM. The anti-HER2 Fab-6His surfaces based on VS-bearing, Carboxyl-EG_6, and NTA-EG_6 chips were prepared according to the above operation. The unreacted VS groups were blocked with a freshly prepared solution of 20 mM 2-aminoethanol (10 mM HEPES, pH 8.0) for 6 h at 25 °C. The flow rate was set at 50 μL/min, and the QCM frequency changes were monitored over time at 25 °C. A blocking step was performed first with 1 mg/mL BSA (10 mM HEPES buffer, pH 7.4) for the three kinds of anti-HER2 Fab-6His surfaces. For adsorption measurements, cell membrane-derived liposome solution was allowed to flow for 15 min, followed by a washing step with HEPES buffer (10 mM, pH 7.4) for 15 min, a regeneration step with 0.01 M NaOH for 10 min, and a final washing step for 10 min with HEPES buffer (10 mM, pH 7.4). The mass of adsorbed protein can be estimated according to the Sauerbrey equation (eq 1).

DOI: 10.1021/acs.langmuir.9b02933
Langmuir 2019, 35, 16466−16475

The adsorption isotherms were studied using a set of cell membrane-derived liposome solutions with different concentrations in the range from 0.8 to 300.0 μg/mL and fitted to the Hill equation (eq 3)

$$R_{eq} = {R_{max}C_{eq}}^{n} / (K_d + {C_{eq}}^{n}) \quad (3)$$

where, R_{eq} is the equilibrium binding mass of cell membrane-derived liposomes, C_{eq} is the concentration of cell membrane-derived liposome when the reaction reaches equilibrium, R_{max} is the maximum binding mass of cell membrane-derived liposome, K_d is the dissociation constant, and n is the Hill coefficient.

RESULTS AND DISCUSSION

Surface Chemistry and XPS Characterization. Due to the strong electron-withdrawing property of sulfone in DVS, one vinyl group in the molecule can be efficiently introduced onto hydroxyl-terminated surfaces through catalytic oxa-Michael reaction,[25] while the other vinyl group (VS) renders high reactivity toward nucleophilic groups even in neutral solution.[27] The starting surface bearing hydroxyl groups, that is, EG_6-OH SAMs, was obtained by the self-assembly of hydroxy-EG_6-undecanethiol on the Au-coated substrates. Oligo(ethylene glycol) on the self-assembly monolayer surfaces provides the terminal hydroxyl group for conjugation while effectively reduces nonspecific protein adsorption.[28] PPh_3 was selected as the catalyst, which could result in a high surface density of VS groups.[29]

The preparation of EG_6-OH SAMs on the cleaned Au-coated substrates and the surface functionalization with DVS were characterized by XPS. The self-assembly and DVS functionalization are illustrated in Figure 1a. The atomic percentages of the surface organic compositions are summarized in Table S1. The XPS spectra of survey scans and high-resolution S 2p are illustrated in Figure 1b,c. The doublet peaks observed at 162 eV with a 2:1 area ratio and a splitting of 1.2 eV of the EG_6-OH surface can be assigned to the thiol species that bind to Au. A doublet peak at 168 eV was observed after DVS modification, which can be assigned to the sulfone groups. These results indicate the successful functionalization of DVS onto the EG_6-OH SAM surface.

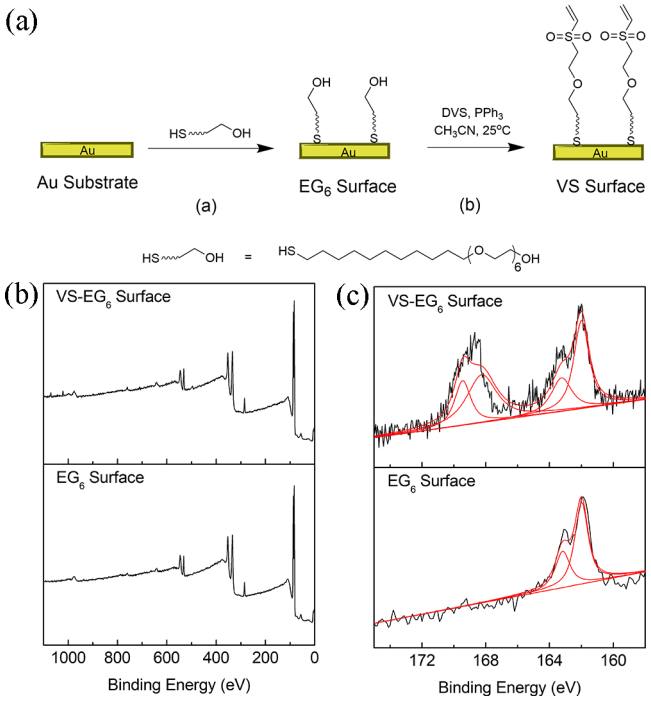

Figure 1. (a) Surface functionalization and (b, c) XPS spectra of survey scans (b) and S 2p (c) for EG_6-OH SAMs and DVS-modified surface.

To enable the specific reaction between amino acids and VS groups on the surface, the α-amino group in histidine and lysine, that is, Boc-His and Boc-Lys, respectively, were protected and Boc-His and Boc-Lys were used for the reaction at different pH (Figure 2a). The surface reactions were characterized by XPS (Figure 2 and Figure S1). The successful conjugation of the two amino acids via either the ε-amino group in Boc-Lys or the imidazole group in Boc-His is expected to introduce nitrogen atoms onto the VS-functionalized SAM surface, resulting in the appearance of a nitrogen signal around 400 eV. As illustrated in Figure 2b,c, the result indicates that the reactivity of the amino acid depends on the solution pH. The signals of N 1s were not detected on the surfaces treated with the acidic solution at pH = 6.5. However, at pH 8.0, both Boc-His and Boc-Lys reacted with the VS-bearing surface. Interestingly, the VS-bearing surfaces exhibit higher reaction selectivity toward the protected histidine at pH 7.0.

To compare the reaction selectivity between N-terminal amine and imidazole of histidine in details, two peptides with free N-terminal amine, that is, RGD and GGGRGDS (pK_a = 6.34), and a protected oligopeptide, that is, Boc-HHHHHH, were selected to react with the VS-EG_6 surface at pH 7.0. The resulting samples were characterized by XPS. The spectra of survey scans and high-resolution scans of C 1s and N 1s are shown in Figure S2. The atomic percentages of nitrogen are summarized in Figure S3. The much weaker yet measurable signals of nitrogen on both RGD and GGGRGDS samples suggest the free N-terminal amine being less reactive than the imidazole residues of Boc-HHHHHH. The result above suggests that the nucleophilicity of the imidazole side chain in histidine is higher than that of the primary amine in lysine and N-terminal amino under neutral conditions.

Solution-Based Reactions of Amino Acids with VS-Bearing Compound. To understand the specificity of the reaction between the VS group and the protected amino acids in details, a mixed solution of Boc-His and Boc-Lys was reacted with VS-EG_3-OMe (synthesis route and chemical structure illustrated in Figure S4) at pH 7.0, and the resulting mixture was analyzed by ^{13}C NMR (Figure 3 and Figure S5). The typical peaks of the vinyl group at 131.5 ppm (Figure 3b, peak A) and 135.7 ppm (Figure 3b, peak B) significantly decreased, indicating the occurrence of the addition reaction. Compared to the spectra of the starting compounds, two new peaks at 137.8 ppm (Figure 3b, peak C) and 40.0 ppm (Figure 3c, peak D) were observed in the spectrum of the resulting mixture. Accordingly, the two peaks belong to the carbon atoms on the imidazole and vinyl groups, respectively. It has been reported that the peak at 39.0 ppm (Figure 3c, peak E) attributed to the ω-carbon atom of lysine shifts to 50.0 ppm once lysine reacted with the VS compound.[30] As expected, the peak at 50 ppm was not detected (Figure 3c), suggesting that the reaction between Boc-Lys and VS-EG_3-OMe did not occur. All the above results are consistent with our XPS results of that VS groups react with Boc-His preferentially at pH 7.0.

Immobilization of HaloTag-6His. The higher reactivity of the surface VS groups toward histidine in the neutral

DOI: 10.1021/acs.langmuir.9b02933
Langmuir 2019, 35, 16466−16475

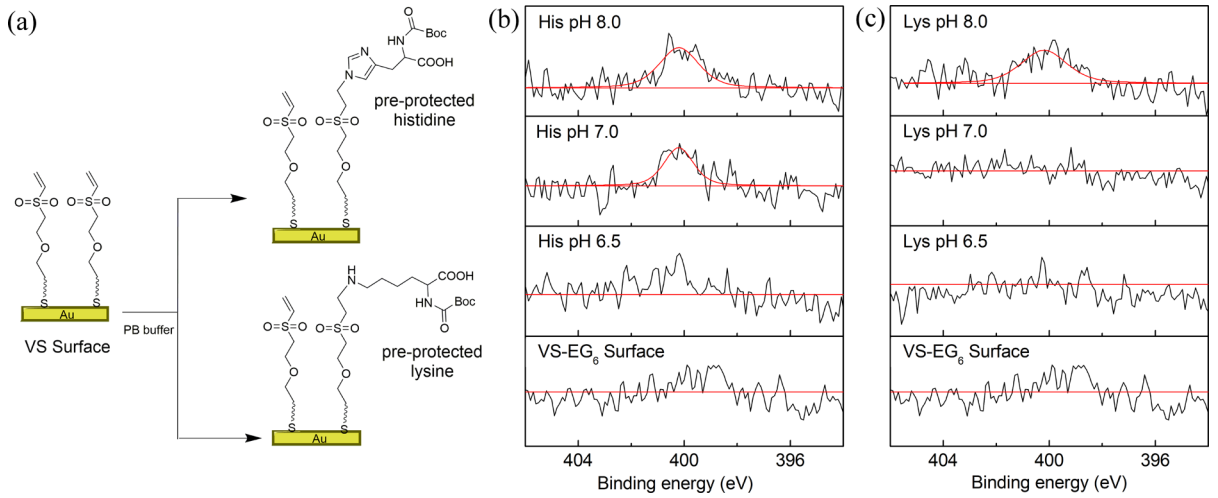

Figure 2. (a) Surface reactions and (b, c) XPS high-resolution of N 1s spectra of VS-EG_6 surfaces treated with the protected amino acids, that is, Boc-His (b) and Boc-Lys (c), in different pH solutions.

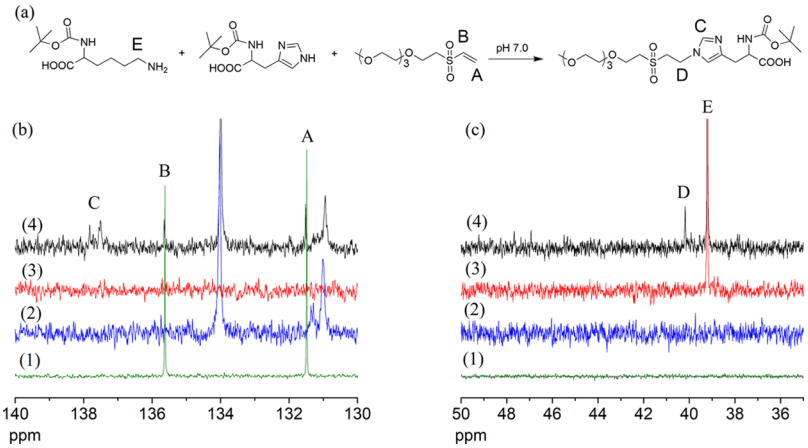

Figure 3. (a) Solution-based reaction and (b, c) the ^{13}C NMR spectra of VS-EG_3-OMe (1), Boc-His (2), Boc-Lys (3) and the resulting products after reaction (4): at (b) 130−140 ppm and the spectra at (c) 35−50 ppm.

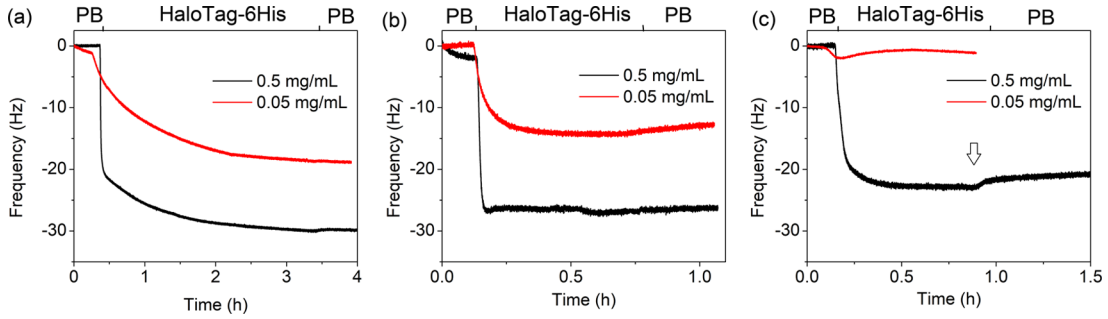

Figure 4. Real-time QCM sensorgrams for HaloTag-6His immobilization onto (a) VS-EG_6, (b) Carboxyl-EG_6, and (c) NTA-EG_6 surfaces by using QCM experiments.

solution provides a promising method for the site-specific immobilization of His-tagged proteins. A model of His-tagged enzyme, HaloTag-6His, was selected to demonstrate the site-specific immobilization onto the VS-bearing surface, that is, the VS-EG_6 surface. Carboxy-EG_6 and NTA-EG_6 surfaces were used as controls, which represent the commonly-used covalent linking and the coordinate linking methods, respectively. The real-time sensorgrams of His-tagged protein immobilization were recorded by QCM and SPR (Figure 4 and Figure S6). For both Carboxy-EG_6 and NTA-EG_6 surfaces, the immobilization processes reached equilibria in approximately 30 min. In contrast, it takes ~180 min on the VS-EG_6 surface, which may be caused by the slower reaction rate. The amounts of the immobilized proteins are summarized in Table 1 and Figure S7. For both low and high protein concentrations (0.05 and 0.5 mg/mL), the amounts of the immobilized proteins on VS-EG_6 and Carboxy-EG_6 surfaces are higher than those on the NTA-EG_6 surface. To exclude nonspecific interactions of HaloTag-6His with the VS-EG_6 surface, two control experiments were carried out. As shown in Figure S8, the nonspecific

DOI: 10.1021/acs.langmuir.9b02933
Langmuir 2019, 35, 16466−16475

Table 1. Molar Density and Calculated Specificity of Immobilized HaloTag-6His and BSA on VS-EG_6, Carboxyl-EG_6, and NTA-EG_6 Surfaces

sample surfaces	HaloTag-6His concentration	HaloTag-6His (pmol/cm^2)	BSA (pmol/cm^2)	calculated specificity (HaloTag-6His/BSA)
VS-EG_6	0.5 mg/mL	15.6	2.2	7.1
	0.05 mg/mL	9.8		
Carboxyl-EG_6	0.5 mg/mL	13.5	5.3	2.5
	0.05 mg/mL	6.5		
NTA-EG_6	0.5 mg/mL	10.6	2.9	3.7
	0.05 mg/mL	0.5		

adsorption onto unfunctionalized EG_6-OH SAMs is negligible. After the VS-EG_6 surface was pretreated with excess Boc-His, HaloTag-6His could not adsorb on the surface (Figure S9). The results clearly show that the VS-EG_6 surface has high binding affinity and specificity toward HaloTag-6His. The high specificity is due to the preference of VS groups toward the imidazole side chain in histidine (Scheme 1d), while the presence of continuous six histidine residues might improve the reaction efficiency to some extent.

It is worth noting that the NTA-EG_6 surface exhibited a lower amount of immobilized His-tagged proteins with a noticeable slow dissociation (indicated by the arrows in Figure 4c). As mentioned above, one of the main drawbacks for the coordinate linking method is due to its intrinsic reversibility. The typical dissociation constants between His-tagged proteins and Ni^{2+}-NTA are reported to be approximately 10^{-6} M.[18,31] In addition, the reversible binding is also very sensitive to imidazole and chelating agents, for example, EDTA, in solution.[32]

Native BSA was selected as a negative control protein that does not have a His-Tag (Figure S10). Among the three types of surfaces, Carboxyl-EG_6 surface showed the highest amount of the immobilized BSA. This is because the NHS-treated carboxyl groups are highly reactive toward ω-amino groups of lysine and N-terminus in BSA. To determine the specificity of immobilization of the different immobilization methods, the ratio of HaloTag-6His to BSA was calculated and listed in Table 1. As expected, the VS-EG_6 surface exhibited the best site-specific immobilization.

To further demonstrate the specificity of surface VS groups toward His-Tag, we selected streptavidin and streptavidin-6His for the immobilization experiments. The resulting surfaces were characterized by XPS. The spectra of survey scans and high-resolution scans of C 1s and N 1s are presented in Figure S11. The atomic percentages of nitrogen are summarized in Figure S12. The significant amounts of streptavidin-6His on both VS-EG_6 and Carboxyl-EG_6 surfaces were observed, which are evidenced by both amide signals of C 1s (~288.2 eV) and nitrogen signals in Figure S11b,c, respectively. We believe that the VS surface exhibits high specificity toward His-Tag under neutral conditions, although some nonspecific adsorption of the protein would also occur to some extent.

Subsequent HRP Immobilization and Detection. HaloTag-6His is a mutant dehalogenase with a molecular weight of ~34 kDa. This enzyme possesses a hydrophobic pocket in which a chlorinated ligand can covalently bind inside.[33] Thus, it is critical to preserve the accessibility of the substrate to the binding site of the enzyme after the immobilization. As illustrated in Figure S13, the His-Tag is located at the opposite position to the binding pocket. Once HaloTag-6His is anchored onto a surface through His-Tag, the binding pocket is expected to be exposed to the solution. A carboxyl-terminated chlorinated ligand (compound **1**) was synthesized (the synthesis route and chemical structures are illustrated in Figure S14) and used as a tracer molecule. The ^{1}H NMR spectrum of the ligand is shown in Figure S15. The carboxyl-terminated chlorinated ligand consists of the following two moieties: (1) a hydrocarbon chain that generates hydrophobic interaction within the binding pocket and (2) an oligo(ethylene oxide) chain that extends the length of the ligand and increases the solubility as well. The ligand was activated by NHS/EDC and covalently linked to horseradish peroxidase (HRP), named as Cl-linked HRP.

A solution-based competitive fluorescence assay was carried out to examine the specific binding between Cl-linked HRP and HaloTag-6His (Figure S16a). A mixture of Cl-linked HRP and HaloTag-6His was incubated at room temperature, followed by addition of the HaloTag coumarin ligand, which is composed of the fluorescent coumarin group and chloroalkane chain. The resulting mixtures were ultrafiltered to remove free the HaloTag coumarin ligand. A mixture of unlabeled HRP and HaloTag-6His was used as a control for HaloTag-6His labeled with the HaloTag coumarin ligand, while the HaloTag coumarin ligand solution in the absence of HaloTag-6His was set as the blank control. The readouts of the fluorescence assay (Figure S16b) indicate that Cl-linked HRP interacted with HaloTag-6His through the specific enzymatic binding.

VS-EG_6, Carboxyl-EG_6, and NTA-EG_6 surfaces were incubated with HaloTag-6His, followed by addition of Cl-linked HRP. The quantity of the bound Cl-linked HRP was examined with TMB assay. The control assay contains unlabeled HRP with the HaloTag-6His/VS-EG_6 surface. As shown in Figure 5a, the low value of the unlabeled HRP sample rules out the nonspecific adsorption of HRP on the surface with the immobilized HaloTag-6His. Consistent with the QCM results, the value of VS-EG_6 surface assay is roughly

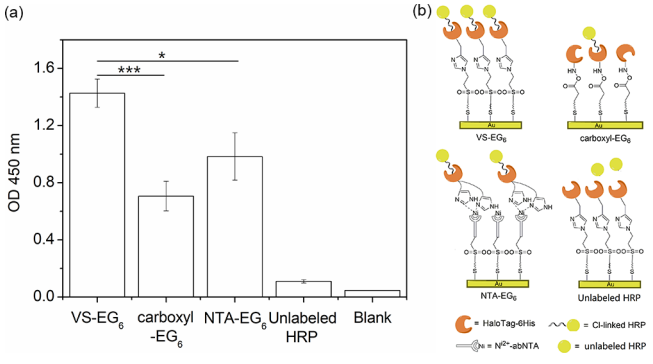

Figure 5. (a) Enzyme-linked assay and (b) proposed orientation of the immobilized HaloTag-6His onto VS-EG_6, Carboxyl-EG_6, and NTA-EG_6 surfaces.

DOI: 10.1021/acs.langmuir.9b02933
Langmuir 2019, 35, 16466−16475

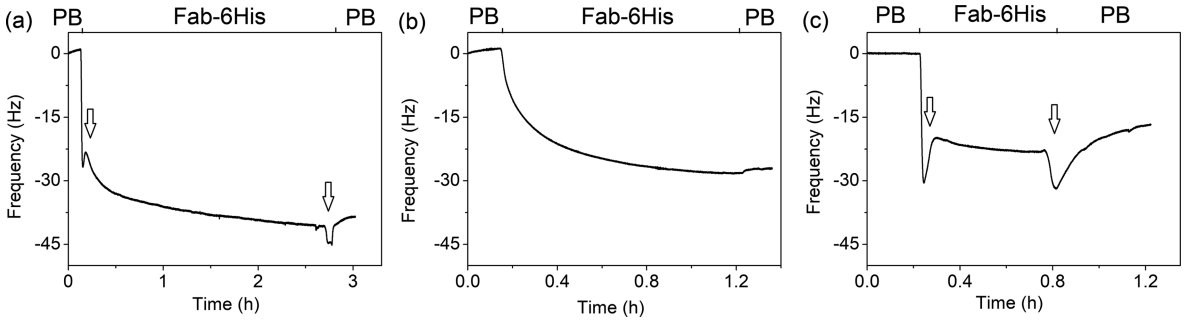

Figure 6. Real-time protein immobilization of anti-HER2 Fab-6His (Fab-6His) onto (a) VS-EG_6, (b) Carboxyl-EG_6, and (c) NTA-EG_6 surfaces by using QCM experiments.

1.5 times that of the NTA-EG_6 surface assay, which suggests that HaloTag-6His is orientated in a similar manner as the coordinate linking method (Figure 5b). As expected, the similar amount of immobilized HaloTag-6His on the Carboxyl-EG_6 surface (close to the VS-EG_6 surface listed in Table 1) did not lead to the similar signal level of the enzyme-linked assay. The result strongly indicates that random immobilization of HaloTag-6His fails to expose the binding pocket for Cl-linked HRP (Figure 5b). All the results above support that our VS immobilization method can achieve site-specific immobilization of HaloTag-6His in a covalent manner, which in turn orientates the binding pocket away from the surface and leads to a higher activity.

Immobilization of Anti-HER2 Fab-6His and Capture of $HER2^+$ Liposome. The orientated antibody is highly desired for all immune assays to achieve a high binding affinity and capacity toward the antigen. Anti-HER2 antibody, a therapeutic monoclonal antibody targeting human epithelial receptor 2 (HER2) that is typically overexpressed on the cell membrane of human cancers, for example, breast and stomach,[34] is used as a model antibody to evaluate the importance of orientated antibody for biosensing. To demonstrate the utility of our site-specific immobilization method, a His-Tag was engineered into the fragment antigen-binding (Fab) of anti-HER2, which is located at the C-terminus of the truncated heavy chain. The sequence of anti-HER2 Fab-6His is illustrated in Experimental Section 3.1, Supporting Information, and the SDS-PAGE analyses of anti-HER2 Fab-6His and anti-HER2 antibody are shown in Figure S17. Fab-6His was expressed in CHO and then purified by using a Protein L affinity column, which would avoid potential contaminants originating from immobilized metal ion affinity chromatography (IMAC) purification.

The real-time bindings of Fab-6His onto VS-EG_6, Carboxyl-EG_6, and NTA-EG_6 surfaces were obtained by QCM (Figure 6). The amounts of the immobilized Fab-6His by different methods are summarized in Table 2. The amounts of the immobilized Fab-6His on different surfaces are 13.6, 9.6, and 5.9 pmol/cm^2 for VS-EG_6, Carboxyl-EG_6, and NTA-EG_6, respectively. The result is highly consistent with the HaloTag-6His immobilization assay. The VS immobilization method exhibits the highest amount of protein immobilization among the three methods. For both the VS immobilization method and the coordinate linking method, the "mass overshoots" can be observed during adsorption and desorption of Fab-6His (indicated by the arrows in Figure 6a,c). It had been reported that the mass overshoots[35,36] are caused by the conformational change or reorientation of the adsorbed proteins. Here, we suppose that the adsorbed proteins would be reoriented on the two surfaces driven by the site-specific immobilization of VS and NTA toward His-Tag, and the significant characteristic peaks of mass overshoots could be attributed to the high molecular weight (~48 kDa) and cylindrical conformation of Fab-6His. It is not surprising that the protein reorientation is absent on the Carboxyl-EG_6 surface due to the quick formation of the permanent covalent bonds between the proteins and NHS-activated carboxyl groups.

Table 2. Molar Density of Immobilized Anti-HER2 Fab-6His and the Values of K_d, R_{max}, and n of $HER2^+$ Liposome Binding on the Three Sample Surfaces

sample surfaces	anti-HER2 Fab-6His (pmol/cm^2)	K_d (μg/mL)	R_{max} (Hz)	n
VS-EG_6	13.6	17.3	95.1	0.63
Carboxyl-EG_6	9.6	52.7	113.9	0.73
NTA-EG_6	5.9	52.0	37.5	1.00

To characterize the antigen-binding ability of three kinds of anti-HER2 Fab-6His surfaces, a HER2 positive cell line, SK-BR-3, was selected for the antigen-binding experiments. The HER2 expression level of SK-BR-3 was confirmed by flow cytometry (Figure S18). To avoid the fast adhesion of mammalian cells on a surface, the liposomes derived from the SK-BR-3 cell line were prepared according to the reported method[8] (hydrodynamic size illustrated in Figure S19).

The binding kinetics of $HER2^+$ liposomes on the anti-HER2 Fab-6His surfaces prepared by VS-EG_6, Carboxyl-EG_6, and NTA-EG_6 methods were monitored in real-time by QCM (Figure 7a–c). The liposomes with a broad range of concentrations from 0.8 to 300.0 μg/mL were examined. The synthetic liposome without the HER2 antigen ($HER2^-$) was used as a negative control for the binding study. The results showed that the amounts of bound synthetic liposomes on the anti-HER2 Fab-6His surface (immobilized by the VS-EG_6 method) (Figure S20) were much lower than that of the $HER2^+$ liposome at both low and high concentrations (5.0 and 25.0 μg/mL), which indicates that the binding of $HER2^+$ liposome onto the anti-HER2 Fab-6His surface is specific. The binding isotherms of $HER2^+$ liposomes (Figure 7d) on the three surfaces were fitted with the Hill equation (eq 3). The values of K_d, R_{max}, and n are calculated and summarized in Table 2. The K_d values of VS-EG_6, Carboxyl-EG_6, and NTA-EG_6 surfaces are 17.3, 52.7, and 52.0 μg/mL, respectively. The binding affinity of $HER2^+$ liposomes toward the anti-HER2 Fab-6His surface prepared by our VS immobilization method is much higher than that of $HER2^+$ liposomes toward the

DOI: 10.1021/acs.langmuir.9b02933
Langmuir 2019, 35, 16466−16475

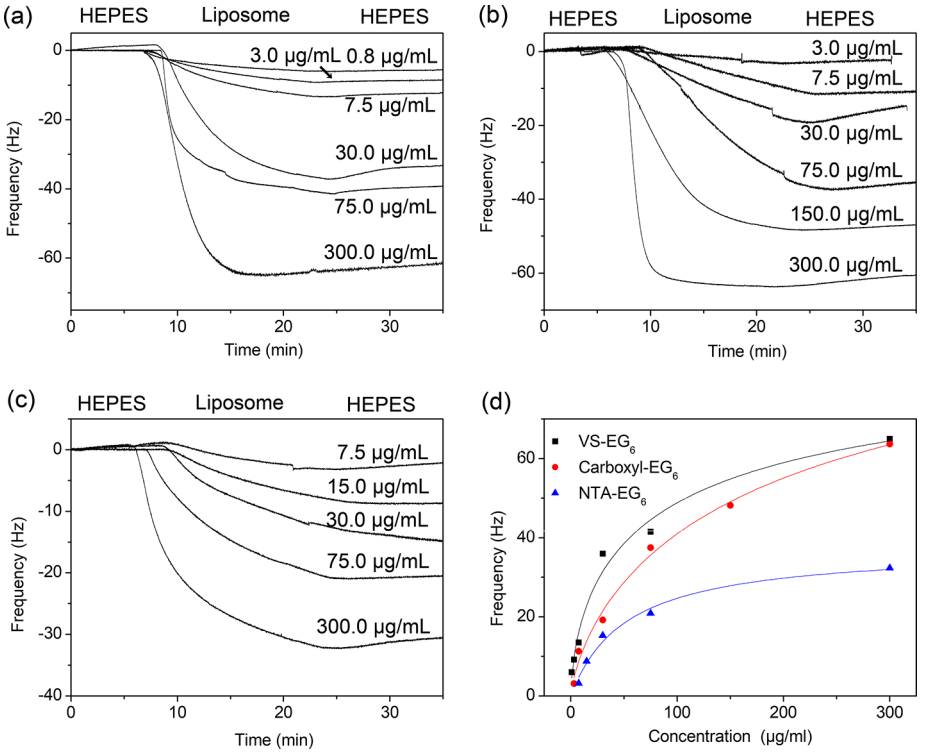

Figure 7. Real-time HER2$^+$ liposome binding experiments onto the anti-HER2 Fab-6His surfaces prepared by (a) VS-EG$_6$, (b) Carboxyl-EG$_6$ and (c) NTA-EG$_6$ methods. (d) Binding isotherms on the three surfaces were calculated.

surfaces prepared by commonly used covalent linking and the coordinate linking methods. The significantly improved affinity is due to the high immobilization efficiency and the larger exposure of the antigen-binding domain through the VS immobilization method. In addition, the limit of detection (LOD) for the HER2$^+$ liposome on the three surfaces was calculated to be 0.15, 1.79, and 4.95 μg/mL, respectively (Figure S21 and Table S2). As expected, the detection sensitivity of the antigen is improved more than 10-fold through the site-specific immobilization.

For the site-directed immobilization of His-tagged proteins, the coordinate linking method has been used in a broad spectrum of biomedical applications. However, the reversible binding between His-Tag and metal ion causes the low immobilization amount and slow but continuous dissociation of His-tagged proteins, which was observed in Figures 4c and 6c. Although the multiple chelators[37] (e.g., bis-, tris, and tetrakis-NTA) have been used to improve the affinities with proteins due to the multivalent interactions, the binding is still very sensitive to the imidazole and metal chelators such as EDTA in solution. Anti-(His-Tag) antibody method[38] is also sensitive to the solution conditions that the dissociation will occur under both acidic and alkaline conditions. Our covalent linking method based on VS-bearing surface not only provides high specificity and immobilization efficiency but also effectively improves the stability of immobilization anchor. The simple preparation method of VS-bearing surface and neutral immobilization conditions also provides advantages for its application. Furthermore, we conjecture the application of this site-specific reaction in the PEGylation of His-tagged proteins.

CONCLUSIONS

In this work, we developed a novel site-specific method for the efficient immobilization of His-tagged proteins. His-tagged proteins were conjugated onto the VS-bearing surface through a covalent linking between His-Ta in the protein and the VS groups on the surface. Both on a surface and in aqueous solution, spectroscopic evidence demonstrated that the reactivity of the imidazole side chain in histidine is higher than that of a primary amine in lysine at pH 7.0. In contrast to the traditional covalent linking (NHS/EDC-activated carboxyl) and coordinate linking methods (Ni^{2+}-NTA), our VS immobilization method results in a much higher amount of protein immobilization with low nonspecific adsorption. The subsequent enzyme-linked assay and HER2$^+$ liposome binding experiment showed that the two His-tagged proteins, that is, HaloTag-6His and anti-HER2 Fab-6His, are orientated on the sample surface through VS/His-Tag covalent bonds, which would in turn expose the binding domains to the solution. According to the HER2$^+$ antigen-binding assay, this new immobilization method provides a much stronger binding affinity with lower LOD. Combined with the ease in the fabrication of VS-bearing surfaces on Au,[25] nanoparticles,[30] and chromatographic resins,[29] our new VS immobilization method paved the way for improving the sensitivity of biosensors and performance of biocatalysts.

ASSOCIATED CONTENT

Supporting Information

The Supporting Information is available free of charge at https://pubs.acs.org/doi/10.1021/acs.langmuir.9b02933.

Experimental section including expression and purification of HaloTag-6His and anti-HER2 Fab-6His, preparation of Cl-linked HRP, protein immobilization

DOI: 10.1021/acs.langmuir.9b02933
Langmuir 2019, 35, 16466−16475

experiments by SPR, and preparation of cell membrane-derived liposomes; XPS spectra and atomic percentage, synthesis route and chemical structure of VS-EG_3-OMe, ^{13}C NMR characterization of solution reaction, real-time sensorgrams and quantification of HaloTag-6His immobilization using SPR, binding behaviors of HaloTag-6His on OEG_6-OH surface and Boc-His blocked VS-EG_6 surface using QCM measurement, real-time sensorgrams of BSA immobilization using QCM, synthesis and ^1H NMR characterization of carboxy-terminated chlorinated ligand, fluorescence assay of a solution-based competitive detection of Cl-linked HRP conjugation with HaloTag-6His, SDS-PAGE analysis of anti-HER2 Fab-6His and antibody, HER2 expression level analysis of SK-BR-3 cells by using flow cytometry, hydrodynamic diameter of cell-derived liposomes, real-time binding experiments of synthesized liposome onto anti-HER2 Fab-6His surface prepared by VS-EG_6 method, calibration plot of frequency versus liposomes concentration, and LOD values of $HER2^+$ liposome on anti-HER2 Fab-6His surfaces (PDF)

AUTHOR INFORMATION

Corresponding Author

*E-mail: ffcheng@dlut.edu.cn.

ORCID

Fang Cheng: 0000-0002-9246-7972
Wei He: 0000-0002-6638-9691
Gang Cheng: 0000-0002-7170-8968
Qing Wang: 0000-0002-1108-3134

Notes

The authors declare no competing financial interest.

ACKNOWLEDGMENTS

This work was supported by the National Key Research and Development Program of China (No. 2018YFA0703000), the National Natural Science Foundation of China (Nos. 21773022 and 31771033), Fundamental Research Funds for the Central Universities (No. DUT16RC(3)019), and Natural Science Foundation of Liaoning Province of China (No. 2019-ZD-0144). F.C. and W.H. acknowledge the State Key Laboratory of Fine Chemicals for support.

REFERENCES

(1) Steen Redeker, E.; Ta, D. T.; Cortens, D.; Billen, B.; Guedens, W.; Adriaensens, P. Protein engineering for directed immobilization. *Bioconjugate Chem.* **2013**, *24*, 1761−1777.

(2) Jasensky, J.; Ferguson, K.; Baria, M.; Zou, X.; McGinnis, R.; Kaneshiro, A.; Badieyan, S.; Wei, S.; Marsh, E. N. G.; Chen, Z. Simultaneous observation of the orientation and activity of surface-immobilized enzymes. *Langmuir* **2018**, *34*, 9133−9140.

(3) Rusmini, F.; Zhong, Z.; Feijen, J. Protein immobilization strategies for protein biochips. *Biomacromolecules* **2007**, *8*, 1775−1789.

(4) Makaraviciute, A.; Ramanaviciene, A. Site-directed antibody immobilization techniques for immunosensors. *Biosens. Bioelectron.* **2013**, *50*, 460−471.

(5) Turková, J. Oriented immobilization of biologically active proteins as a tool for revealing protein interactions and function. *J. Chromatogr. B: Biomed. Sci. Appl.* **1999**, *722*, 11−31.

(6) Mustafaoglu, N.; Alves, N. J.; Bilgicer, B. Oriented immobilization of Fab fragments by site-specific biotinylation at the conserved nucleotide binding site for enhanced antigen detection. *Langmuir* **2015**, *31*, 9728−9736.

(7) Chen, S.; Liu, L.; Zhou, J.; Jiang, S. Controlling antibody orientation on charged self-assembled monolayers. *Langmuir* **2003**, *19*, 2859−2864.

(8) Wang, X.; Wang, M.; Lei, R.; Zhu, S. F.; Zhao, Y.; Chen, C. Chiral surface of nanoparticles determines the orientation of adsorbed transferrin and its interaction with receptors. *ACS Nano* **2017**, *11*, 4606−4616.

(9) Lou, D.; Ji, L.; Fan, L.; Ji, Y.; Gu, N.; Zhang, Y. Antibody-oriented strategy and mechanism for the preparation of fluorescent nanoprobes for fast and sensitive immunodetection. *Langmuir* **2019**, *35*, 4860−4867.

(10) Lin, P.-H.; Huang, S.-C.; Chen, K.-P.; Li, B.-R.; Li, Y.-K. Effective construction of a high-capacity boronic acid layer on a quartz crystal microbalance chip for high-density antibody immobilization. *Sensors* **2019**, *19*, 28−37.

(11) Duval, F.; van Beek, T. A.; Zuilhof, H. Key steps towards the oriented immobilization of antibodies using boronic acids. *Analyst* **2015**, *140*, 6467−6472.

(12) Zhou, Y.; Guo, T.; Tang, G.; Wu, H.; Wong, N.-K.; Pan, Z. Site-selective protein immobilization by covalent modification of GST fusion proteins. *Bioconjugate Chem.* **2014**, *25*, 1911−1915.

(13) Engin, S.; Trouillet, V.; Franz, C. M.; Welle, A.; Bruns, M.; Wedlich, D. Benzylguanine thiol self-assembled monolayers for the immobilization of SNAP-tag proteins on microcontact-printed surface structures. *Langmuir* **2010**, *26*, 6097−6101.

(14) Shen, L.; Schroeder, M.; Ogorzalek, T. L.; Yang, P.; Wu, F.-G.; Marsh, E. N. G.; Chen, Z. Surface orientation control of site-specifically immobilized nitroreductase (NfsB). *Langmuir* **2014**, *30*, 5930−5938.

(15) Li, X.; Song, S.; Pei, Y.; Dong, H.; Aastrup, T.; Pei, Z. Oriented and reversible immobilization of His-tagged proteins on two- and three-dimensional surfaces for study of protein−protein interactions by a QCM biosensor. *Sens. Actuators, B* **2016**, *224*, 814−822.

(16) Gao, X.; Li, Y.; Qin, Y.; Chen, E.; Li, Q.; Zhao, X.; Bian, L.; Zheng, J.; Li, Z.; Zhang, Y.; Zheng, X. Reversible and oriented immobilization of histidine-tagged protein on silica gel characterized by frontal analysis. *RSC Adv.* **2015**, *5*, 24449−24454.

(17) Xia, S.; Cartron, M.; Morby, J.; Bryant, D. A.; Hunter, C. N.; Leggett, G. J. Fabrication of nanometer- and micrometer-scale protein structures by site-specific immobilization of histidine-tagged proteins to aminosiloxane films with photoremovable protein-resistant protecting groups. *Langmuir* **2016**, *32*, 1818−1827.

(18) Zhao, X.; Li, Q.; Xiao, C.; Zhang, Y.; Bian, L.; Zheng, J.; Zheng, X.; Li, Z.; Zhang, Y.; Fan, T. Oriented immobilisation of histidine-tagged protein and its application in exploring interactions between ligands and proteins. *Anal. Bioanal. Chem.* **2014**, *406*, 2975−2985.

(19) Včeláková, K.; Zusková, I.; Kenndler, E.; Gaš, B. Determination of cationic mobilities and pK_a values of 22 amino acids by capillary zone electrophoresis. *Electrophoresis* **2004**, *25*, 309−317.

(20) Peciak, K.; Laurine, E.; Tommasi, R.; Choi, J. W.; Brocchini, S. Site-selective protein conjugation at histidine. *Chem. Sci.* **2019**, *10*, 427−439.

(21) Mather, B. D.; Viswanathan, K.; Miller, K. M.; Long, T. E. Michael addition reactions in macromolecular design for emerging technologies. *Prog. Polym. Sci.* **2006**, *31*, 487−531.

(22) Gmach, J.; Joachimiak, Ł.; Błażewska, K. M. Aza-michael addition of imidazole analogues. *Synthesis* **2016**, *48*, 2681−2704.

(23) Cong, Y.; Pawlisz, E.; Bryant, P.; Balan, S.; Laurine, E.; Tommasi, R.; Singh, R.; Dubey, S.; Peciak, K.; Bird, M.; Sivasankar, A.; Swierkosz, J.; Muroni, M.; Heidelberger, S.; Farys, M.; Khayrzad, F.; Edwards, J.; Badescu, G.; Hodgson, I.; Heise, C.; Somavarapu, S.; Liddell, J.; Powell, K.; Zloh, M.; Choi, J.-w.; Godwin, A.; Brocchini, S. Site-specific PEGylation at histidine tags. *Bioconjugate Chem.* **2012**, *23*, 248−263.

(24) Jia, S.; He, D.; Chang, C. J. Bioinspired thiophosphorodichloridate reagents for chemoselective histidine bioconjugation. *J. Am. Chem. Soc.* **2019**, *141*, 7294−7301.

DOI: 10.1021/acs.langmuir.9b02933
Langmuir 2019, 35, 16466−16475

(25) Cheng, F.; Li, M.; Zhao, X.; Wang, H.; He, W.; Hua, X.; Wang, Q.; Qu, J. Controllable functionalization of hydroxyl-terminated self-assembled monolayers via catalytic oxa-Michael reaction. *Biointerphases* **2018**, *13*, No. 06E407.
(26) Fang, C.; Mingyang, L.; Wei, H.; Hanqi, W. Control of the ligand surface density through reaction kinetics of amino and surface vinyl sulfone groups. *Acta Phys.-Chim. Sin.* **2018**, *34*, 177−184.
(27) Wang, H.; Cheng, F.; Li, M.; Peng, W.; Qu, J. Reactivity and kinetics of vinyl sulfone-functionalized self-assembled monolayers for bioactive ligand immobilization. *Langmuir* **2015**, *31*, 3413−3421.
(28) Rodriguez Emmenegger, C.; Brynda, E.; Riedel, T.; Sedlakova, Z.; Houska, M.; Alles, A. B. Interaction of blood plasma with antifouling surfaces. *Langmuir* **2009**, *25*, 6328−6333.
(29) Cheng, F.; Li, M.; He, W.; Sun, B.; Qin, J.; Qu, J. Activation of resin with controllable ligand density via catalytic oxa-Michael addition and application in antibody purification. *J. Chromatogr. A* **2018**, *1570*, 1−9.
(30) Wang, H.; Cheng, F.; Shen, W.; Cheng, G.; Zhao, J.; Peng, W.; Qu, J. Amino acid-based anti-fouling functionalization of silica nanoparticles using divinyl sulfone. *Acta Biomater.* **2016**, *40*, 273−281.
(31) Arnold, F. H. Metal-affinity separations: a new dimension in protein processing. *Bio/technology* **1991**, *9*, 151−156.
(32) Ericsson, E. M.; Enander, K.; Bui, L.; Lundström, I.; Konradsson, P.; Liedberg, B. Site-specific and covalent attachment of his-tagged proteins by chelation assisted photoimmobilization: a strategy for microarraying of protein ligands. *Langmuir* **2013**, *29*, 11687−11694.
(33) England, C. G.; Luo, H.; Cai, W. HaloTag technology: a versatile platform for biomedical applications. *Bioconjugate Chem.* **2015**, *26*, 975−986.
(34) Truffi, M.; Colombo, M.; Sorrentino, L.; Pandolfi, L.; Mazzucchelli, S.; Pappalardo, F.; Pacini, C.; Allevi, R.; Bonizzi, A.; Corsi, F.; Prosperi, D. Multivalent exposure of trastuzumab on iron oxide nanoparticles improves antitumor potential and reduces resistance in HER2-positive breast cancer cells. *Sci. Rep.* **2018**, *8*, 6563−6573.
(35) Sun, L.; Frykholm, K.; Fornander, L. H.; Svedhem, S.; Westerlund, F.; Åkerman, B. Sensing conformational changes in DNA upon ligand binding using QCM-D. Polyamine condensation and Rad51 extension of DNA layers. *J. Phys. Chem. B* **2014**, *118*, 11895−11904.
(36) Cheng, F.; Li, M.-Y.; Wang, H.-Q.; Lin, D.-Q.; Qu, J.-P. Antibody-ligand interactions for hydrophobic charge-induction chromatography: a surface plasmon resonance study. *Langmuir* **2015**, *31*, 3422−3430.
(37) You, C.; Piehler, J. Multivalent chelators for spatially and temporally controlled protein functionalization. *Anal. Bioanal. Chem.* **2014**, *406*, 3345−3357.
(38) Sasakura, Y.; Kanda, K.; Yoshimura-Suzuki, T.; Matsui, T.; Fukuzono, S.; Han, M. H.; Shimizu, T. Protein microarray system for detecting protein-protein interactions using an anti-His-Tag antibody and fluorescence scanning: effects of the heme redox state on protein-protein interactions of heme-regulated phosphodiesterase from *escherichia coli*. *Anal. Chem.* **2004**, *76*, 6521−6527.

DOI: 10.1021/acs.langmuir.9b02933
Langmuir 2019, 35, 16466−16475